

Original Research

Integrated Single-Cell and Transcriptome Sequencing Analyses Develop a Ubiquitination-Associated Signature in Gastric Cancer and Identified OTULIN as a Novel Biomarker

Zhongting Huang^{1,*}, Zhiyong Zhang¹, Yangyang Tu¹, Haibin He¹, Feng Qiu¹,
Hailong Qian¹, Chunshu Pan^{2,*}¹Department of Gastrointestinal Surgery, Ningbo Medical Center Lihuli Hospital, The Affiliated Lihuli Hospital, Ningbo University, 315000 Ningbo, Zhejiang, China²Department of Radiology, Ningbo No.2 Hospital, 315000 Ningbo, Zhejiang, China*Correspondence: lhluangzhongting@nmbu.edu.cn (Zhongting Huang); panchunshu@nimte.ac.cn (Chunshu Pan)

Academic Editor: Feng Jiang

Submitted: 12 April 2023 Revised: 24 June 2023 Accepted: 10 July 2023 Published: 27 November 2023

Abstract

Background: Gastric cancer (GC) is the most commonly diagnosed digestive system malignancy with a dismal survival outcome. The prognostic value of ubiquitination-related genes (URGs) in GC has yet to be discovered. **Methods:** Two GC cohort datasets were obtained from the Cancer Genome Atlas Program (TCGA) and Gene Expression Omnibus (GEO) databases. Stepwise Cox analysis was employed to generate a signature. Then, we applied unsupervised clustering analysis to determine subclusters in GC based on URGs. Single-cell analysis was carried out to depict the cellular location of model genes. The CIBERSORT method was performed to estimate the immune landscape. Finally, preliminary wet lab work was utilized to disclose the potential effect of OTULIN. **Results:** Our proposed signature was set up based on five URGs (*OTULIN*, *UBE2C*, *USP1*, *USP2*, and *MAPT*) which could serve as a risk classifier to categorize GC cases. In addition, it was demonstrated that the ubiquitination-associated model could depict the immune landscape and forecast immunotherapy response for GC patients. Furthermore, *in vitro* experiments determined the function and effect of OUTLIN in GC. We observed that the knockdown of OUTLIN could suppress cell viability and metastatic ability of GC cell lines. **Conclusions:** Our data lays the groundwork for a comprehensive investigation into the role of URGs in GC and determined OTULIN as a candidate GC biomarker.

Keywords: gastric cancer; ubiquitination; prognosis; immunotherapy response; OTULIN

1. Introduction

Gastric cancer (GC) is a common malignant neoplasm of the digestive system. It has the fourth-highest incidence and the second-highest mortality rate in the world. With the continuous improvement of treatment, the mortality rate of GC has decreased worldwide [1]. However, the survival outcome of GC cases is dismal as the mechanisms affecting prognosis are still unclear. Consequently, the further investigation of molecular mechanisms involved in the occurrence, development, and prognosis of gastric cancer and the search for valuable molecular markers is critical.

Recent studies have shown that the tumor microenvironment (TME) plays a central role in the development of tumors. The TME is a complex system consisting of low oxygen, low pH, high pressure, and a large number of growth factors and protein hydrolases, which regulate a variety of tumor biological behaviors [2]. The TME consists of tumor cells, stromal cells, and an extracellular matrix. The local homeostatic environment, composed of fibroblasts, immune cells, some endothelial cells, and an extracellular matrix, allows for tumor development, invasion, and metastasis [3]. A suitable microenvironment is the “soil” for tumor growth, which can cause genomic instability, pro-

vide scaffolds and barriers, generate immune regions, induce bidirectional differentiation and form a permissive microenvironment, and promote the formation and development of tumors [4,5]. Therefore, it is crucial to focus on the TME to illuminate the mechanisms of GC tumorigenesis.

Post-translational modification (PTM) refers to the covalent processing of proteins during or after translation, where a modification group is attached to one or several amino acid residues or removed by protein hydrolysis, thereby changing the properties of the protein. PTM is widely found in eukaryotic cells and is second only to replication, transcription, and translation as an important regulatory mechanism with biological functions [6]. Several hundred post-translational modifications have been identified, including phosphorylation, ubiquitination, crotonylation, glycosylation, carboxylation, acetylation, lactylation, and ribosylation. The ubiquitin system consists of a complex cascade of reactions, mainly ubiquitin-activating enzyme (E1), ubiquitin-conjugating enzyme (E2), and ubiquitin ligase enzyme (E3), which are involved in the regulation of protein activity, eukaryotic cell cycle, DNA repair, and apoptosis [7,8].



The development and evolution of malignant tumors is a multifactorial induced multi-stage evolutionary process involving numerous mutational accumulations of genes; by activating proto-oncogenes and inactivating oncogenes, their temporal, spatial, quantitative, and qualitative abnormal expression products act on cell growth, differentiation, and apoptosis. It is well known that cells are the basic units of life, and the dynamic changes of protein networks and their related functions are important for life processes [9]. The ubiquitin-proteasome system (UPS) and the lysosomal system are the two major modes of protein degradation and quality control. The ubiquitin-mediated protein degradation system is an important protein quality control system in cells, which regulates cell viability, signaling, and other cellular physiological processes [10].

Numerous studies have demonstrated that ubiquitination-related genes (URGs) are significantly associated with tumorigenesis. For example, in melanoma, the ubiquitination of galectin-3 by RNF8 via K48-linked polyubiquitin chains. Inhibiting galectin-3 restored cytokine levels and immune cell infiltration, providing a potential option for the management of melanoma [11]. Tian *et al.* [12] revealed that USP46 could facilitate cell migration by upregulating ENO1 in esophageal cancer. Nevertheless, the association between UGRs and the prognosis of GC is unknown, making it challenging to exploit ubiquitination-related therapy for GC.

Our study aims to provide insight into the expression pattern of URGs and their regulatory mechanisms in GC in order to determine novel and powerful prognostic biomarkers of GC.

2. Materials and Methods

2.1 Data Collection

The expression profiling and clinical traits of 375 GC samples were downloaded from the TCGA website (<https://portal.gdc.cancer.gov/>). Another GC-independent dataset (GSE84437) containing transcriptome data and survival information was obtained from the Gene Expression Omnibus (GEO) database (<https://www.ncbi.nlm.nih.gov/geo/>). All raw data were pre-processed with the limma package in R software (4.1.3, R Foundation for Statistical Computing, Vienna, Austria). The exclusion criteria were set as follows: (1) histologic diagnosis was not GC; (2) samples without completed data for analysis; and (3) overall survival (OS) time of less than 30 days. We screened the list of UGRs using a relevance score greater than 10.0 from the GENECARDS database website (<https://www.genecards.org/>). Detailed information on these URGs is shown in **Supplementary Table 1**.

2.2 Construction of the Ubiquitination-Associated Signature (UAS)

Firstly, we selected the TCGA dataset as a training set for model establishment. All UGRs were analyzed by univariate Cox regression to screen out prognosis-related URGs ($p < 0.05$). Multivariate analysis was utilized to generate a prognostic model based on the candidate genes from univariate Cox regression. Each GC sample's risk value was generated using the following formula: $\sum_{i=1}^n coef_i * expression\ level\ of\ UAG_i$. The coef represents the coefficient of each UAG calculated by multivariate Cox analyses. The GC cases were divided into high- and low-risk groups according to the median risk value.

2.3 Consensus Gene Clustering

We applied unsupervised clustering through the 'ConsensusClusterPlus' package [13]. The optimal cluster value was determined based on the similarity between the expression matrix of UAGs and the fuzzy clustering measurement ratio.

2.4 Single-Cell RNA Analysis

We obtained scRNA data (GSE167297) of GC from the GEO database. The scRNA-seq matrix for individual samples was analyzed using the Read10x algorithm of the 'Seurat' package [14]. Low-quality cells with ≤ 300 detected genes or $\geq 10\%$ mitochondrial genes were removed and normalized by 'NormalizeData', the top 1500 highly variable genes were then identified by the 'FindVariableFeatures' function. Data quality control and normalization were performed by 'NormalizedData'. The t-SNE method was used to reduce data dimensionality and obtain different cell clusters. All cell populations were annotated using 'FindAllMarkers' based on the cell surface markers.

2.5 Gene Set Enrichment Analysis (GSEA)

GSEA was conducted using GSEA software (version 4.0.1, Massachusetts Institute of Technology, and Regents of the University of California, CA, USA) with 1000 rows. Hallmark and KEGG terms were selected as the target gene sets from MSigDB. Total GC cases were divided into two groups based on risk and enriched for the above gene sets. Any gene set with FDR < 0.25 and $p < 0.05$ was regarded as significant.

2.6 Clinical Potency Investigation

CIBERSORT (<https://cibersort.stanford.edu/>) is an algorithm that estimates the abundance of cell types infiltrated by patients with tumors based on gene expression data [15]. Moreover, single sample gene set enrichment analysis (ssGSEA) was employed to immune activity and function between two risk groups. The drug sensitivity analysis was conducted by the 'pRRophetic' package to detect which drugs presented different sensitivities among the two risk groups. The half-maximal inhibitory concentration (IC50) was calculated to evaluate the drug sensitivity [16].

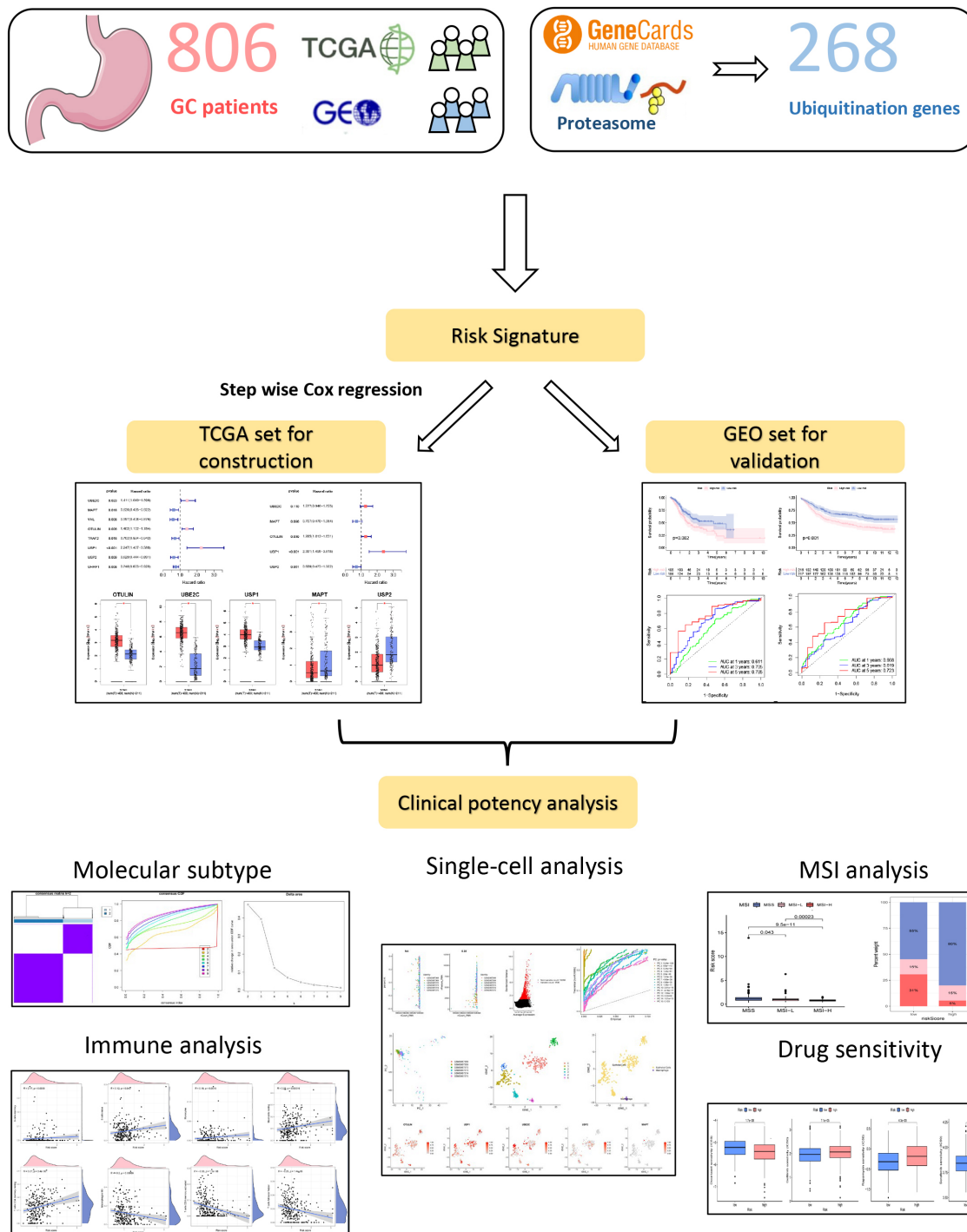


Fig. 1. A flowchart of the present research. Gastric cancer (GC), The Cancer Genome Atlas Program (TCGA), Gene Expression Omnibus (GEO), microsatellite instability (MSI).

2.7 Cell Culture and Transfection

Two human GC cell lines (SGC7901 and BGC823) and one normal gastric epithelium cell line (GES-1) were purchased from the Cell Center of Shanghai Institutes. All cell lines were cultured in RPMI 1640 medium (Invitrogen) containing 10% fetal bovine serum and 1% antibiotics (100 U/mL penicillin G and 100 mg/mL streptomycin) at

37 °C with 5% CO₂. The silencing RNA against OTULIN (si-OTULIN) was synthesized and purchased from RIBBIO (Guangzhou, China). The sequence of si-OTULIN is shown in **Supplementary Table 2**. Lipofectamine 3000 (Invitrogen) was used for cell transfection. Cell lines were authenticated by the Shanghai Biowing Applied Biotechnology Co.,Ltd and Procell Life Science & Technology

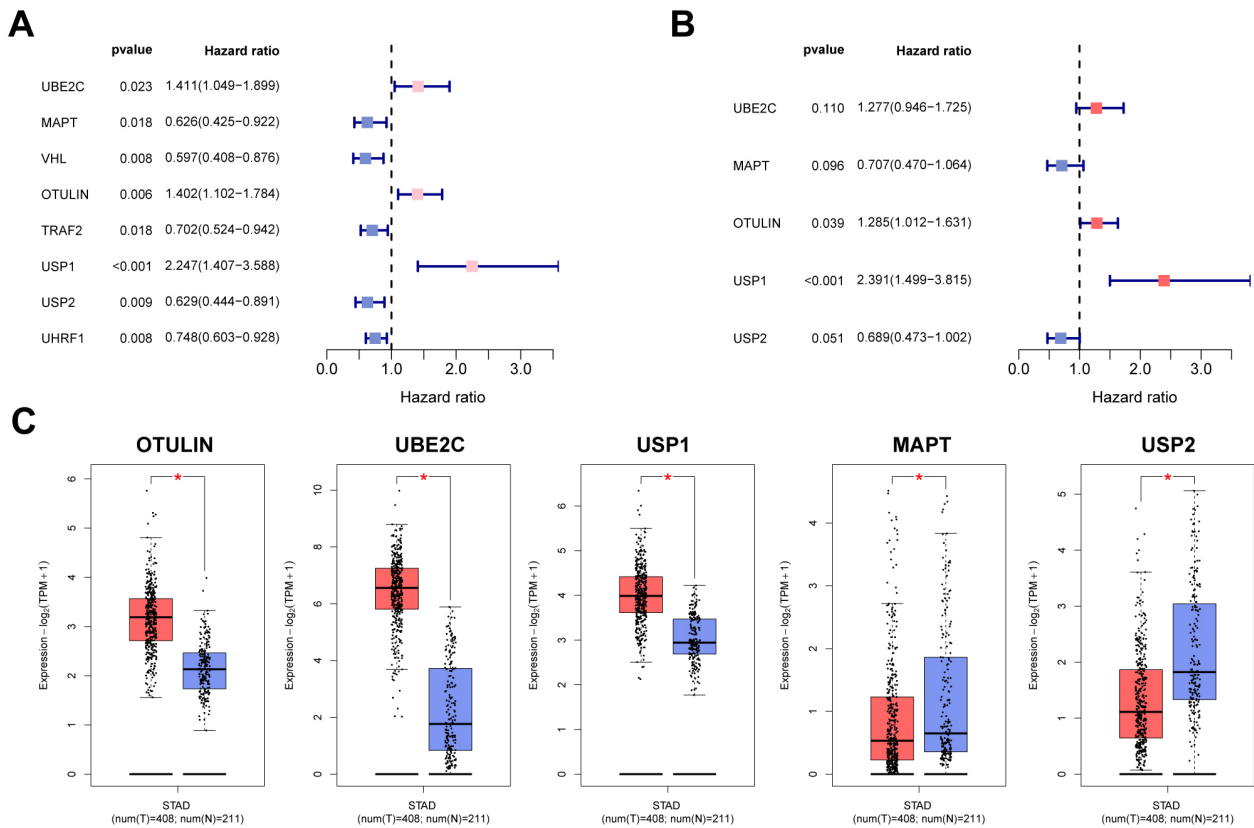


Fig. 2. Construction process of the ubiquitination-associated signature (UAS). (A) Univariate Cox analysis. (B) Multivariate Cox analysis for screening model genes. (C) The expression patterns of UAS genes in gastric cancer (GC) and normal specimens. * $p < 0.05$.

Co.,Ltd. using Short Tandem Repeat profiling (PCR Amplification Kit, Corning, New York, USA). Mycoplasma test was performed in all cell lines every other week using the Mycoplasma PCR Detection Kit (Beyotime, Shanghai, China). Only mycoplasma-free cell lines were used.

2.8 Reverse Transcription-Polymerase Chain Reaction (RT-PCR)

Total RNA was extracted from cells using RNA easy reagent (Vazyme, Nanjing, China) based on the manufacturer's instructions. RNA was then synthesized to cDNA by Primerscript Mix (Takara Bio, Kusatsu, Shiga, Japan). RT-PCR was applied on a Steponeplus system with SYBR Green Regent (Takara Bio, Japan). The relative expression was calculated using the $2^{-\Delta\Delta CT}$ method. The primer sequences of the genes are shown in **Supplementary Table 2**.

2.9 Cell Viability Assay

A total of 10,000 cells per well were seeded into a 96-well plate. After 24 hours of incubation at 37 °C, cell viability was determined by detecting ATP levels in cell lysates using the CellTiter-Glo (CTG) Assay.

2.10 Colony-Formation Assay

A total of 200 cells/well were seeded into six-well plates and incubated for 1-week. Clones were fixed with methanol and stained with 0.1% crystal violet (Servicebio, Wuhan, China) when visible to the naked eye. Image-J (version 1.5b, LOCI, University of Wisconsin, Madison, WI, USA) was used for colony counting.

2.11 EdU Assay

EdU assay was performed to evaluate cell proliferation. The cells were cultured in 96-well plates (5000 cells per well) with complete medium for 24 h. After a 2 h incubation with EdU solution (50 μ M), all cells were fixed and stained with 1 \times Apollo® solution for 30 min. Finally, nuclei were stained with 1 \times Hoechst33342.

2.12 Statistical Analysis

All bioinformatics data were analyzed by R software (version 4.0, Lucent Technologies, Murray Hill, NJ, USA) and wet lab experimental data were analyzed using GraphPad 9.4 (GraphPad Software, Inc., San Diego, CA, USA). Survival curves were used to compare survival differences between the two groups using the Kaplan-Meier (KM) method. The discrepancies in clinical outcomes between groups were examined using the Kaplan-Meier survival

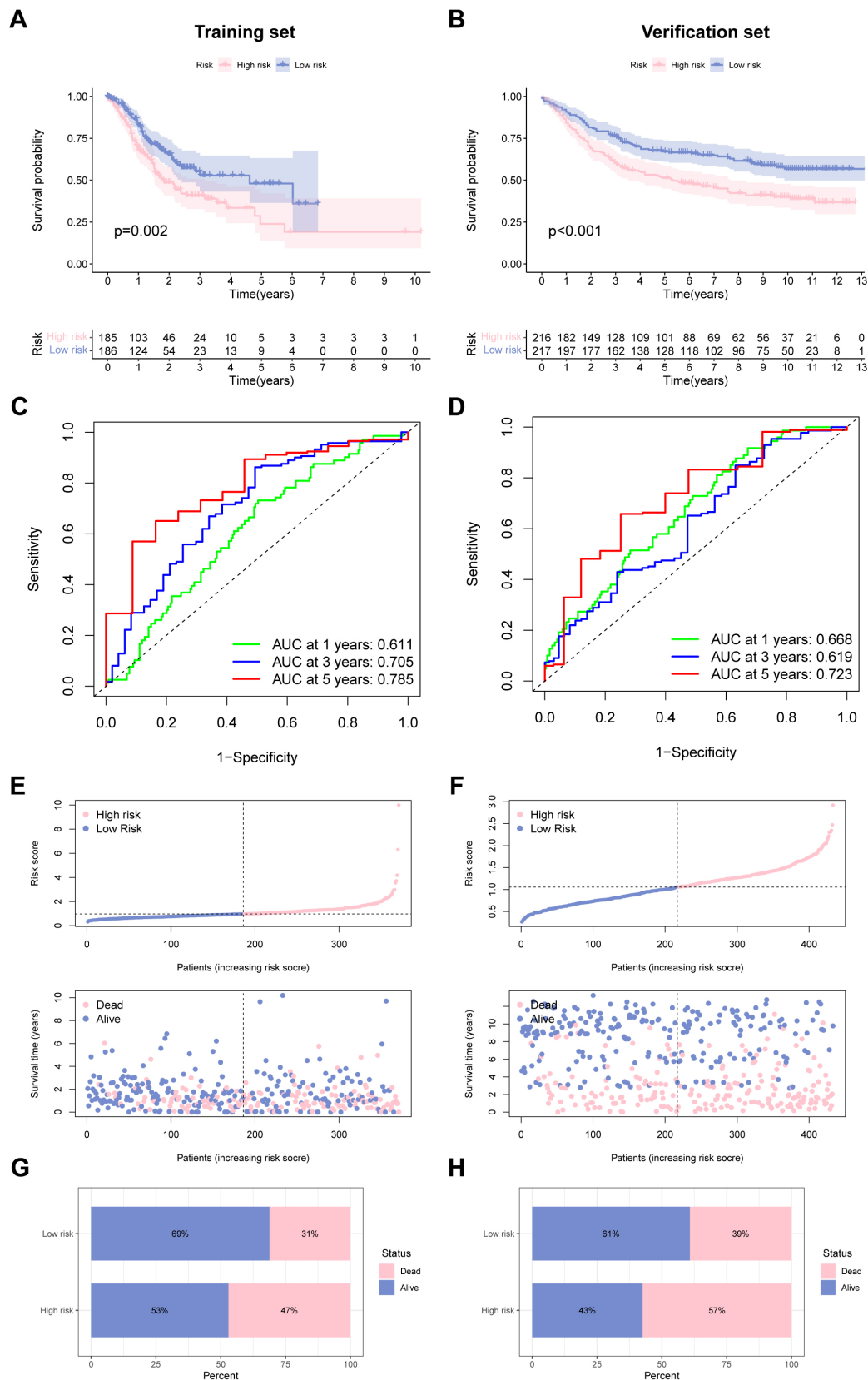


Fig. 3. Performance of the ubiquitination-associated signature. (A,B) Survival curves of survival outcome of GC cases between two groups in the training and verification sets. (C,D) Receiver operating characteristic (ROC) curves to predict the performance of UAS in the two GC cohorts. (E,F) Demonstration of the UAS based on the risk score of the training and verification sets, respectively. (G,H) The proportion of deaths and survival in two subgroups. ROC, receiver operator characteristic.

analysis. Receiver operator characteristic (ROC) curves were plotted to confirm the accuracy of UAS. Cox regression was utilized to detect the independent performance of UAS in GC.

3. Results

3.1 Development of the Ubiquitination-Associated Signature (UAS)

A flowchart of the present research is shown in Fig. 1. Firstly, univariate Cox analysis was employed to obtain eight potential URGs with significant prognosis values, which were then enrolled into the multivariate Cox method (Fig. 2A). Using stepwise Cox methods, we set up the UAS including five URGs (*OTULIN*, *UBE2C*, *USP1*, *USP2*, and *MAPT*) (Fig. 2B). The risk model equation was: $(0.2508 \times \text{OTULIN}) + (0.2446 \times \text{UBE2C}) + (0.87167 \times \text{USP1}) + (-0.3729 \times \text{USP2}) + (-0.3461 \times \text{MAPT})$. Fig. 2C revealed that these URGs were significantly differentially expressed in GC and normal tissues using the GEPIA2 portal. It was shown that *OTULIN*, *USP1*, and *UBE2C* were overexpressed in GC specimens, whereas *USP2* and *MAPT* were upregulated in normal tissues.

3.2 Verification of the UAS

Based on model risk scores constructed from five URGs, we divided GC cases into high- and low-risk groups, showing good predictive ability of the model in both the training and validation groups, and defined them as a USA-high cohort and UAS-low cohort. Survival curves demonstrated that high-risk score was associated with dismal OS in the training set (TCGA cohort), which was confirmed by the verification set (GSE84437) (Fig. 3A,B). The 1-, 3- and 5-year area under the curves (AUCs) were 0.611, 0.705, and 0.785 for the training set (Fig. 3C), 0.668, 0.619, and 0.723 for the verification set (Fig. 3D), respectively, indicating the beneficial predictive ability of our constructed UAS. Fig. 3E,F illustrates the relationship between risk scores and the pattern of patient survival status (alive or dead) distribution. Mortality was significantly decreased in the UAS-low cohort than in the USA-high cohort; both were independent datasets (Fig. 3G,H).

3.3 Independent Prognosis Analysis of the UAS

We employed Cox regression to detect the independent prognostic score of UAS in GC patients. Fig. 4A revealed that univariate analysis remarkably associated the UAS-high score with dismal survival outcomes. Multivariate Cox indicated that the UAS score remained meaningful for forecasting prognosis. In addition, the prognostic independence of UAS was confirmed in the test cohort (Fig. 4C,D). Additionally, we observed that UAS could forecast survival outcomes of different clinical subgroups in terms of age (≤ 65 , $n = 197$ samples, > 65 , $n = 241$ samples), gender (male, $n = 285$ samples, female, $n = 158$ sam-

ples), grade (grade 1–2, $n = 171$ samples, grade 3, $n = 263$ samples) and stage (stage I–II, $n = 189$ samples, stage III–IV, $n = 227$ samples) (Fig. 4E).

3.4 Determination of Ubiquitination-Based Molecular Subtype

To develop a novel molecular subtype in GC, consensus clustering analysis was employed based on 268 URGs. According to the cumulative distribution function (CDF), we conducted the tracking plot from $k = 2$ to 9, where $k = 2$ was identified as the cluster number to divide patients into cluster A ($n = 304$) and cluster B ($n = 504$) (Fig. 5A). Principal component analysis (PCA) indicated that two clusters of GC cases could be effectively distinguished by our proposed novel molecular subtype (**Supplementary Fig. 1A**). Cluster B had a better outcome than cluster A. There was an obvious difference discrepancy in immunocyte infiltration between the two subgroups (Fig. 5B,C). **Supplementary Fig. 1B** summarizes the relationship between UAS-based molecular clusters and different clinical traits. We then identified potential pathways (ubiquitination, DNA repair, and cell cycle) in which clusters might be involved by KEGG enrichment analysis (Fig. 5D).

3.5 Immune Landscape of GC Patients

Next, we applied CIBERSORT and ssGSEA analyses to explore the ability of the model to predict the immune microenvironment of GC patients. In Fig. 6A, B cells memory, B cells naive, monocytes, mast cells resting, and T cells CD4 memory resting positively correlated with risk score, whereas macrophages M0, T cells CD4 memory activated, and T cells follicular helper were negatively correlated with risk score. The results from ssGSEA revealed that immune functions such as CCR, major histocompatibility complex (MHC) class I, and type II interferon (IFN) response differed significantly among the two groups (Fig. 6B). Fig. 6C shows the expression patterns of classical immune checkpoints among two groups. It was shown that CD86, CD200, CD40, NRP1, CD48, CD27, and TNFSF15 were upregulated in the UAS-high group, whereas in the UAS-high group, other immune checkpoints exhibited a decreased expression level.

3.6 Clinical Potency of the UAS

Considering the crucial regulatory role of m6A regulators in GC progression, we determined the relationship between risk score and the expression of m6A regulators. We found that ZC3H13 and FTO were highly expressed in the UAS-high group. In contrast, HNRNPC, ALKBH5, YTHDF2, RBM15, YTHDF1, and METTL3 were downregulated in the UAS-high group (Fig. 7A). There were significant differences in the expression of chemoradiotherapy sensitivity-related genes between the two groups. As shown in Fig. 7B, AKR1C1, EGFR, FLT3, and KIT were significantly overexpressed in the UAS-high group

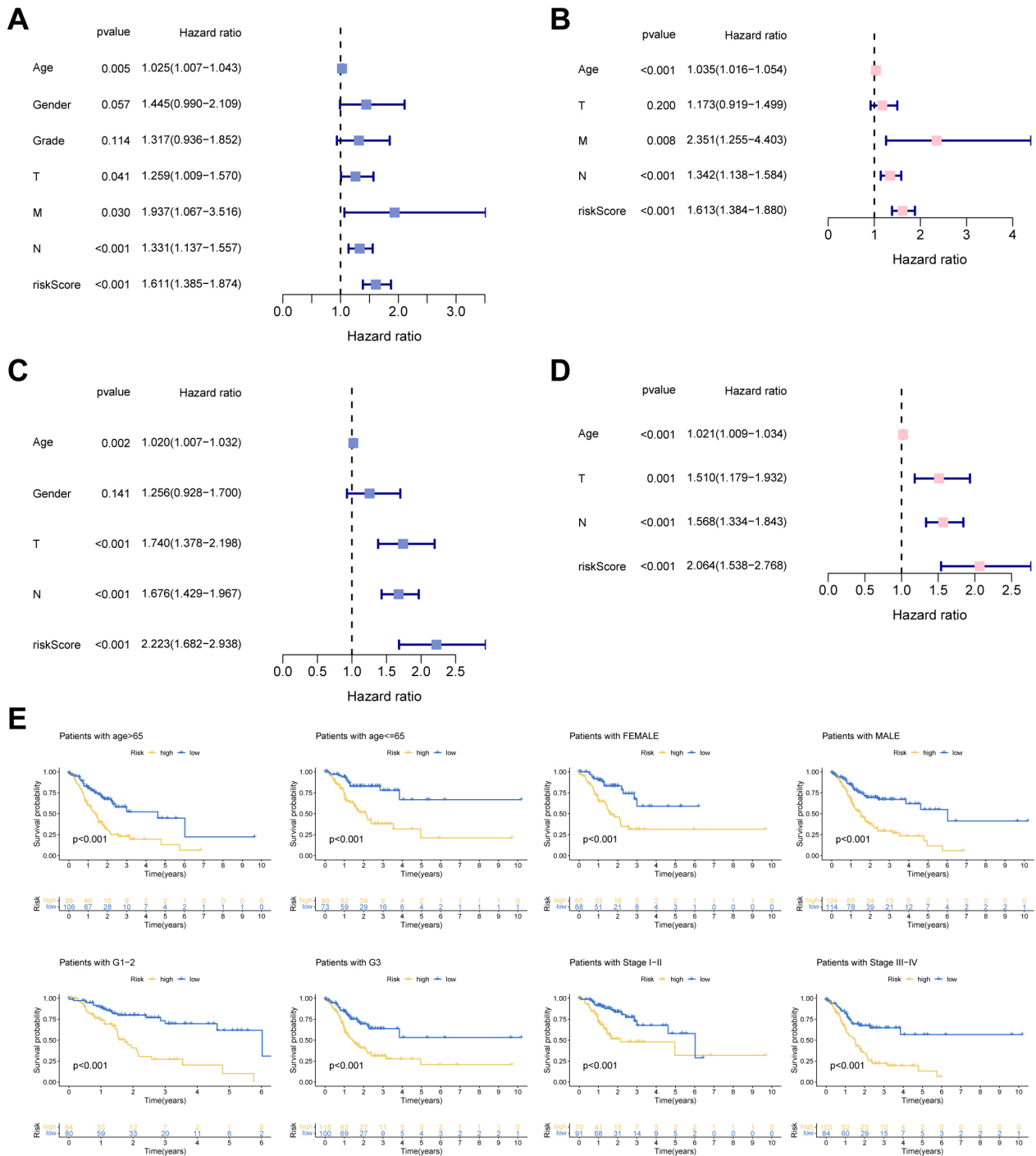


Fig. 4. Independent prognosis analysis. (A,C) Univariate Cox analysis. (B,D) Multivariate Cox analysis. (E) Subgroup survival analysis of the UAS in terms of age, gender, grade, and stage.

(Fig. 7B). The proportion of patients with MSS was significantly lower in the UAS-low cohort than in the UAS-high cohort. In comparison, the proportion of MSI-H was significantly higher in UAS-high cohort (Fig. 7C). In addition, the risk score was negatively correlated with RNA stemness score (RNAss) (Fig. 7D). Drug sensitivity analysis revealed that docetaxel ($p = 1.7 \times 10^{-8}$) had a lower IC50 value in the high-risk cohort, whereas the other three

drugs displayed a higher IC50 value in the high-risk cohort ($p = 7.1 \times 10^{-5}$ for gefitinib, $p = 4.3 \times 10^{-9}$ for rapamycin, $p = 4.4 \times 10^{-9}$ for sorafenib) (Fig. 7E).

3.7 Single-Cell Analysis of the UAS

Subsequently, we detected the expression pattern of five model genes at the single-cell level. A total of 14 GC samples from GSE167297 were enrolled into single-

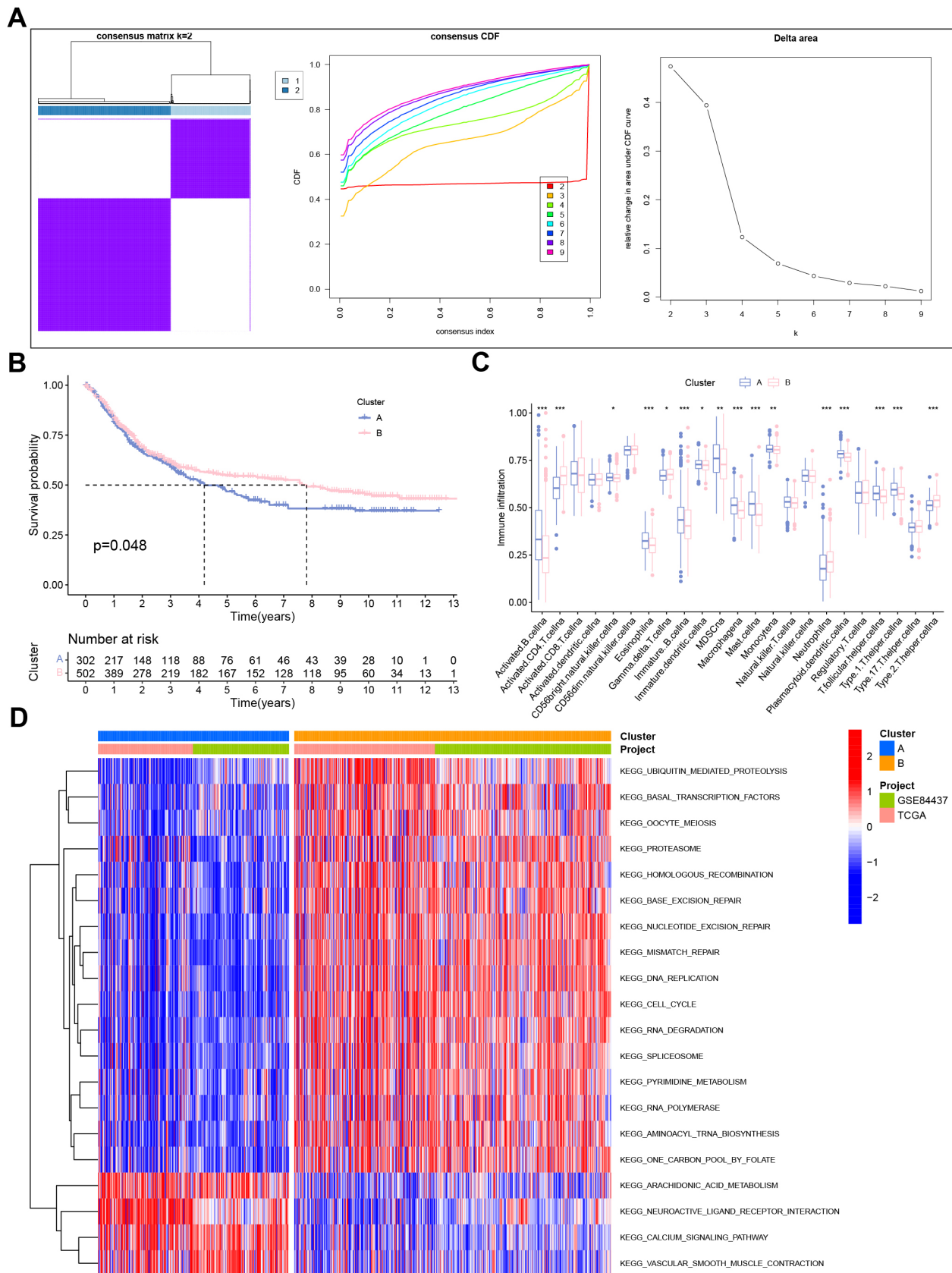


Fig. 5. Cluster analysis for determination of URGs-based molecular subtype. (A) Consensus clustering results. (B) Survival analysis and (C) immune infiltration analysis between two clusters. (D) Gene set variation analysis (GSVA) based on Kyoto Encyclopedia of Genes and Genomes (KEGG) pathway enrichment. * $p < 0.05$; ** $p < 0.01$; *** $p < 0.001$. URGs, ubiquitination-related genes.

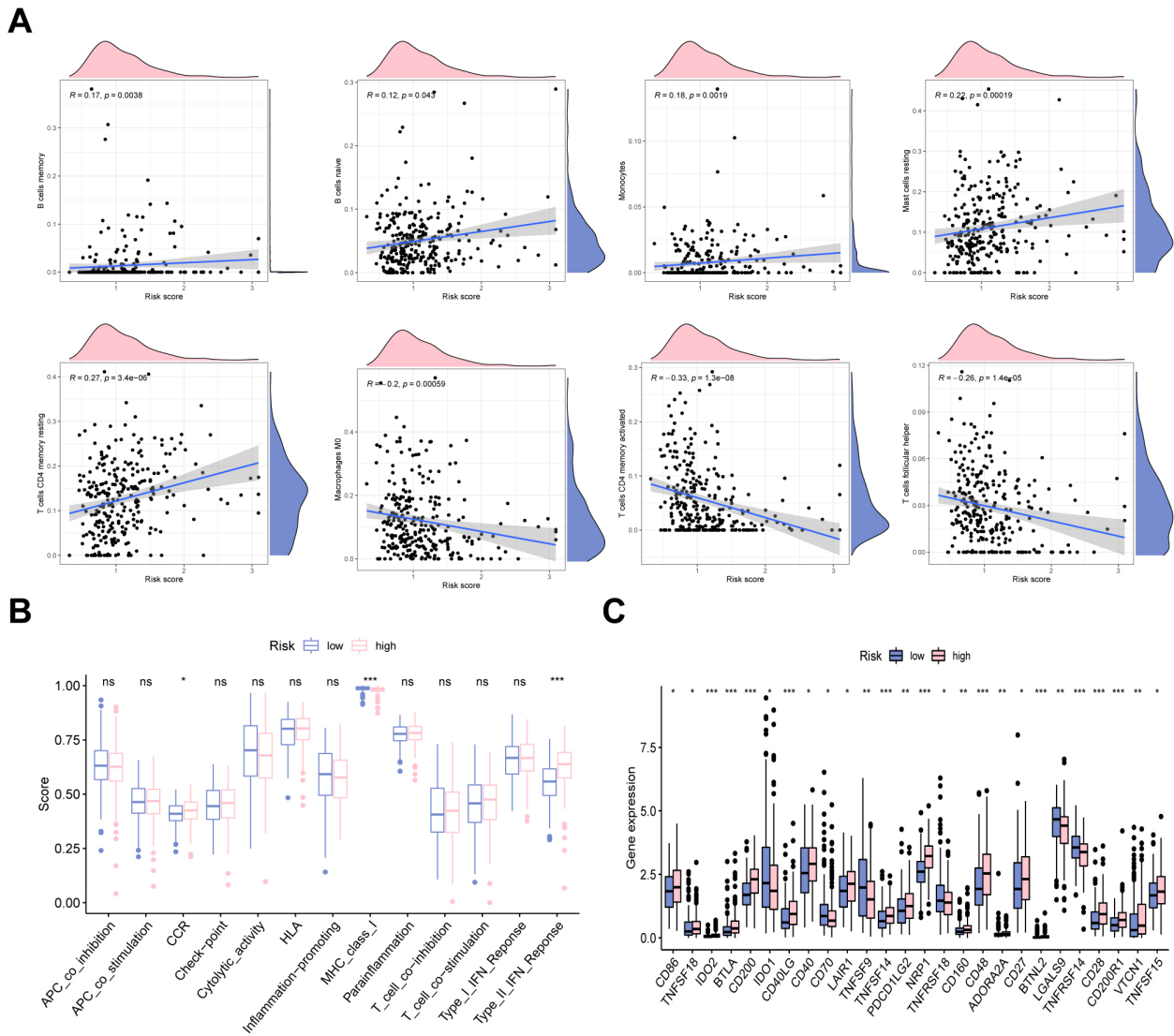


Fig. 6. Immune landscape analysis. (A) The correlation between risk score and immune cells. (B) The difference in immune functions in two risk groups. (C) Immune checkpoints analysis of the UAS. * $p < 0.05$; ** $p < 0.01$; *** $p < 0.001$, ns, no significance.

cell analysis (**Supplementary Fig. 2A**). The top 1500 variable genes with red labels were collected (Fig. 8A). Fig. 8B revealed a favorable integration effect between cluster all samples and 50 PC groups. PCA analysis showed the distribution of all GC cases with no significant batch effects (**Supplementary Fig. 2B**). Using t-SNE diagrams, a total of 30,365 cells were identified and further clustered into 20 different subpopulations (Fig. 8C). Based on the surface marker, we determined 8 cell population types including B cells, dendritic cells (DCs) endothelial cells, epithelial cells, monocytes, NK cells, smooth muscle cells and T cells (Fig. 8D). Next, the cellular location of five URGs was detected. We observed that OTULIN, USP1, and UBE2C were enriched in malignant epithelial cells, whereas USP2 and MAPT were downregulated in malignant epithelial cells (Fig. 8E).

3.8 Identification of OTULIN as a Novel Oncogenic Player in GC

We selected OTULIN to verify our proposed model by various *in vitro* experiments. Fig. 9A shows that OTULIN, USP1, and UBE2C were highly expressed in GC cell lines, whereas USP2 and MAPT were highly expressed in the GES-1 cell line. A PCR assay was carried out to confirm the transfection efficiency of siRNA-OTULIN and OTULIN (Fig. 9B). CTG assay, colony formation, and EdU assay were applied to evaluate the cell viability in GC cells. Cell proliferation was significantly inhibited following the silencing of OTULIN in SGC7901 cells (Fig. 9C–E).

4. Discussion

Ubiquitination is a common post-translational protein modification that serves an important role in tumor development and progression. Ubiquitination is a double-edged

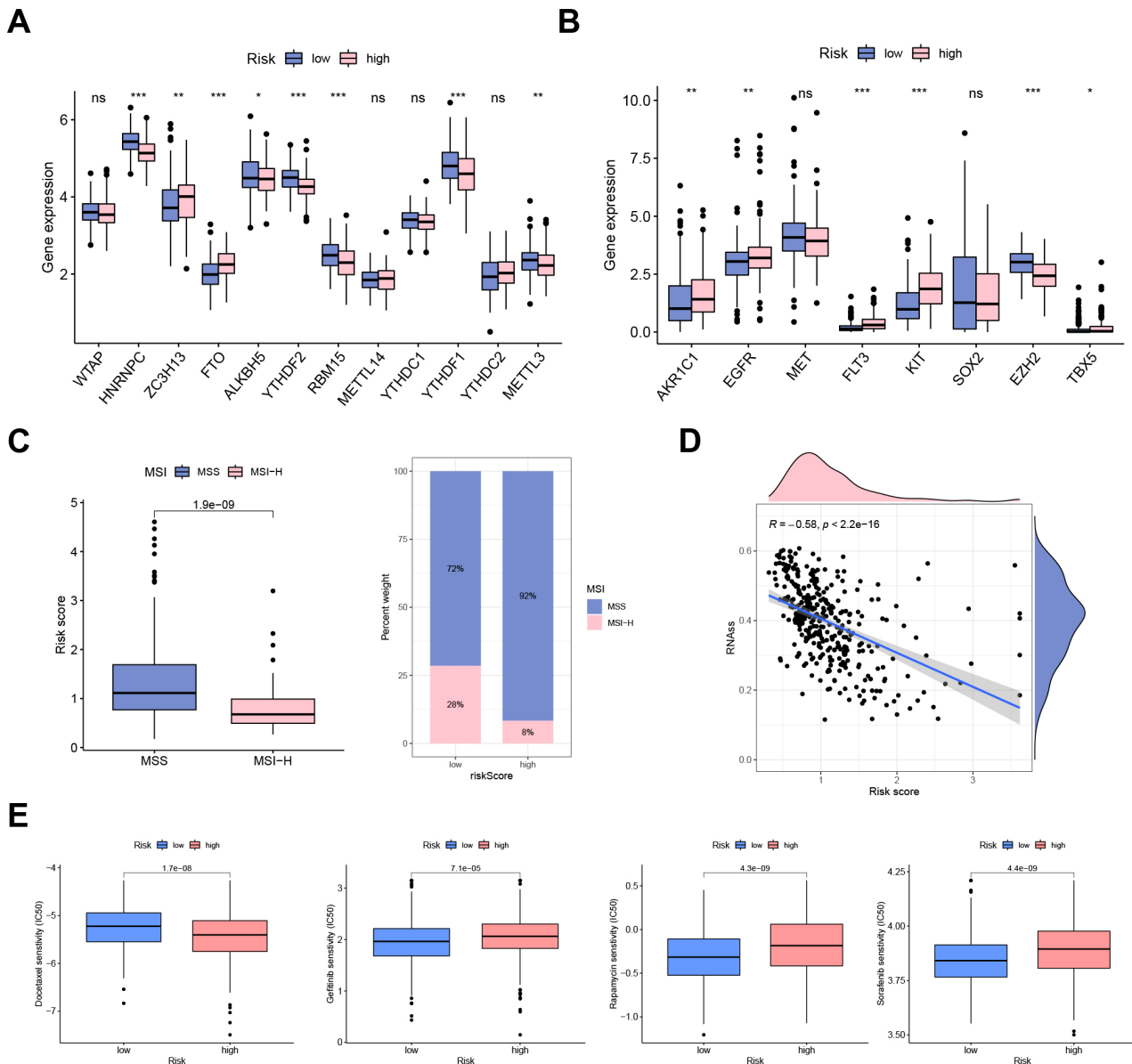


Fig. 7. Clinical potency of the UAS. (A) The expression patterns of m6A regulators and (B) chemosensitivity-related genes between risk groups. (C) Correlation between MSI and risk score. (D) Cancer stemness analysis. (E) Drug sensitivity analysis (docetaxel, gefitinib, rapamycin, and sorafenib). * $p < 0.05$; ** $p < 0.01$; *** $p < 0.001$, ns, no significance.

sword in regulating cancer progression, as the substrate protein might be either an oncogene or a tumor suppressor [17]. For instance, RNF139 was reported to induce cell apoptosis and block glioma cell survival by targeting the AKT pathway [18]. However, OTUD6A, as a tumor driver, could boost cell growth and progression of prostate cancer by stabilizing c-Myc [19]. The dual role of different ubiquitination members in tumors deserves a comprehensive analysis and exploration in GC. Multigene-based signatures have gained more attention due to their robust predictive accuracy over traditional clinical scores [20,21]. Nevertheless, biomarkers with prognosis values based on URGs expression data were not well studied in GC.

Our project aimed to develop a prognostic model based on URGs. We first screen out eight prognostic URGs and further establish a risk model containing five URGs by step Cox analysis. Survival curves illustrated that GC cases in the high-UAS group presented a dismal survival outcome compared to the low-UAS group. The AUC value of ROC curves verified the favorable predictive power of the UAS. Moreover, the results were further verified in the verification cohort. Subsequently, our proposed UAS was demonstrated to be an independent prognostic factor associated with unfavorable OS in different GC subgroups.

Our constructed model was composed of five URGs (*UBE2C*, *MAPT*, *OTULIN*, *USP1*, and *USP2*), all of which have previously been shown to be associated with tumor

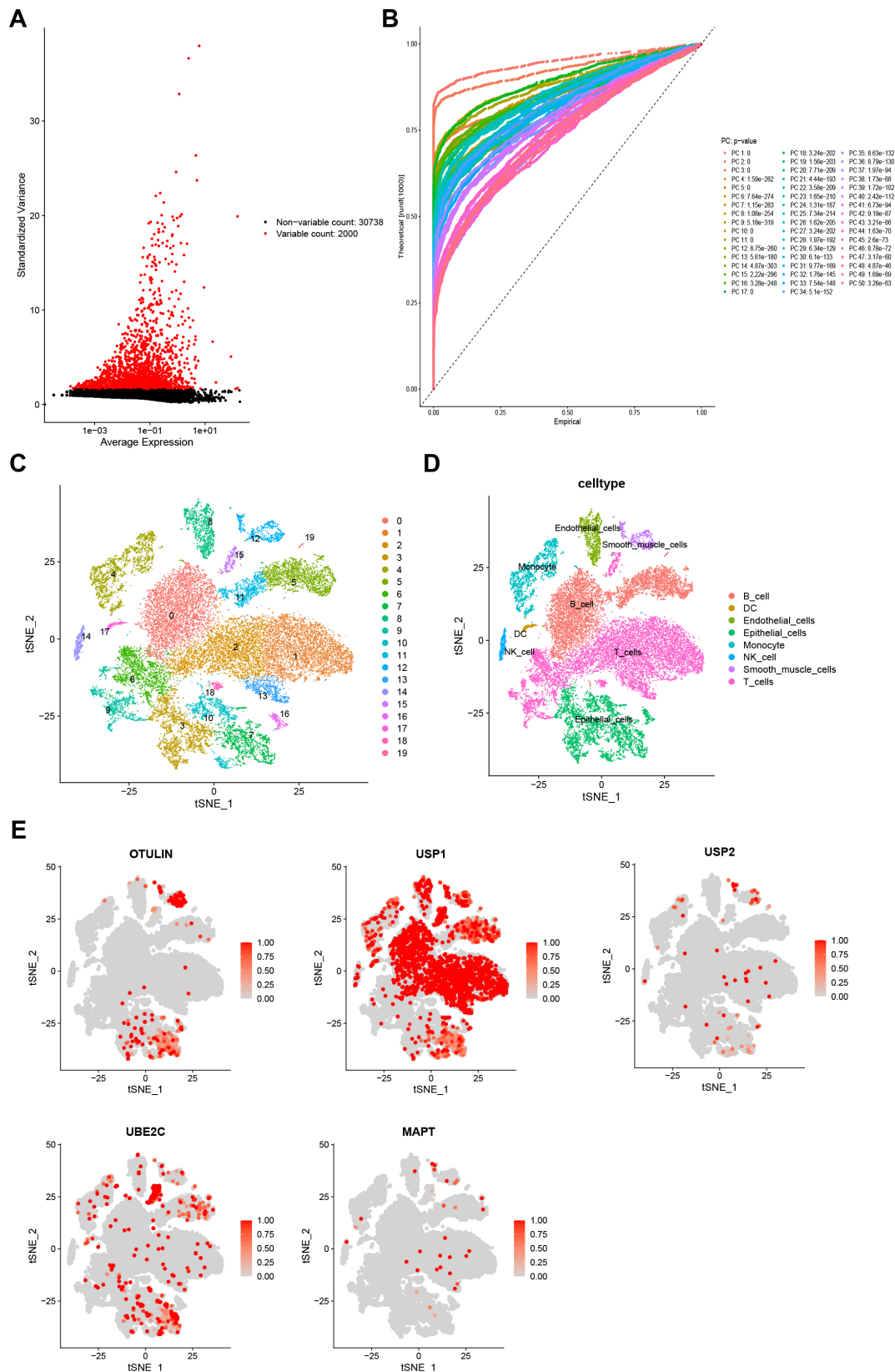


Fig. 8. Single-cell sequencing analysis. (A) A total of the top 1500 variable genes with red labels. (B) Data integration and dimensionality reduction. (C) All cells were clustered into 20 subclusters. (D) Classification of all cells into B cells, dendritic cells (DCs), endothelial cells, epithelial cells, monocytes, NK cells, smooth muscle cells, and T cells. (E) Cellular location of five URGs (*OTULIN*, *USP1*, *USP2*, *UBE2C*, and *MAPT*).

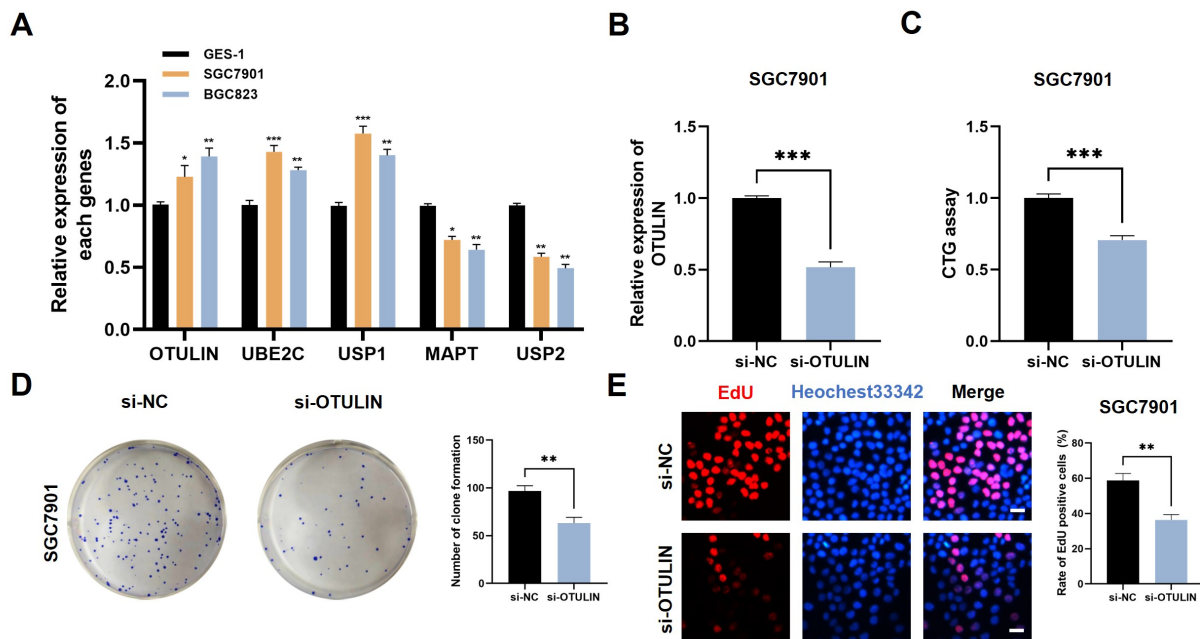


Fig. 9. Identification of OTULIN as a novel oncogenic player in GC. (A) Expression patterns of five model genes in different cell lines were detected by Real-Time Quantitative Reverse Transcription PCR (qRT-PCR) assay. (B) PCR assay indicates the favorable transfection efficiency in GC cell lines. Cell proliferation in different treatment groups was evaluated by (C) CTG assay, (D) colony formation, and (E) EdU assay. Scale bar = 200 μm . * $p < 0.05$; ** $p < 0.01$; *** $p < 0.001$. CTG, CellTiter-Glo.

survival and progression [22,23]. UBE2C, a key component of the ubiquitin-proteasome system, was demonstrated to promote ubiquitination and degrade cyclins. Together with E3 ligases, it acts in the anaphase-promoting complex (APC/C) to regulate the spindle assembly test site [24]. As revealed by Zhang *et al.* [25], UBE2C was highly expressed in GC specimens at both mRNA and protein levels. Meanwhile, UBE2C expression was observed to be associated with lymphatic metastasis and TNM stage. Moreover, Cox-relevant analyses indicated that UBE2C presented prognostic independence in GC [25]. In breast cancer (BC), silencing UBE2C could significantly inhibit cell survival by targeting the mTOR signaling pathway, suggesting UBE2C is expected to be a potential target for the management of BC [26]. OTULIN, a linear deubiquitinating enzyme, plays a central part in pathophysiological effects, including cancer, cell death, vascular regeneration, and neuroinflammation [27]. Wang *et al.* [28] demonstrated that OTULIN could facilitate cell migration and invasion and confer drug resistance to BC by triggering Wnt/ β -catenin signaling. As a classical member deubiquitinating enzyme, numerous reports have disclosed that USP1 exerts a tumor driver in various tumors, including GC, BC, and osteosarcoma [29–31]. For example, Li *et al.* [30] found that USP1 could boost GC cell metastasis through deubiquitination of ID2. Consistent with the above findings, our analysis also indicated that UBE2C, OTULIN, and USP1 were high-risk genes in GC (hazard ratio (HR) = 1.227 for UBE2C, HR = 1.285 for OTULIN, and HR = 2.391 for USP1). Conversely, MAPT

and USP2 were protective genes in GC (HR = 0.707 for MAPT and HR = 0.689 for USP2). Wu *et al.* [32] reported that the knockdown of MAPT could induce chemosensitivity in GC cells. In addition, USP2 also could suppress lung cancer survival through the stabilization of the ARID2 protein [33].

Immune checkpoints (ICPs) are a group of immunosuppressive molecules expressed on immunocytes that play an important role in protecting against autoimmune effects through modulation of immune activation [34]. ICP molecule overexpression contributes to the suppression of immune function and thus encourages the immune escape of tumors. Our data revealed that the majority of ICPs were upregulated in the high-UAS group, which may be an important contributor to their poor prognosis.

In addition to expressing specific antigens that the immune system can recognize, tumor cells also express a variety of immunosuppressive ligands that can bind to inhibitory receptors expressed by T cells. BTLA, like other immune checkpoint molecules (e.g., PD1, CTLA-4, Tim3), inhibits T-cell activity upon binding to the corresponding ligands, leading to tumor immune escape [35]. According to the available experimental analysis, anti-PD1/PD-L1 tumor immunotherapy is effective in specific patients only, with an overall response rate of about 30%. In contrast, the combination of anti-BTLA immunotherapy can improve tumor control and promote cytokine secretion in the body. This may indicate that BTLA, as a suppressive immune checkpoint, is also involved in tumor im-

immune escape [36,37]. NRP1 operates in various tumor cell functions and microenvironments and is an important promoter of tumor development. NRP1, as a member of the NRP family, is mainly expressed in vascular endothelial tissue and interacts with vascular endothelial growth factor (VEGF) to regulate tumor cell invasion, proliferation, promote tumor cell inflammatory response, immune response, and stem cell proliferation processes [38]. CD200, also known as OX2, is a transmembrane glycoprotein with two extracellular immunoglobulin structural domains and an intracellular structure consisting of an unknown signaling domain of 19 amino acids. In addition to familiar hematologic tumors, it was upregulated in multiple solid tumors, including solid tumors such as ovarian cancer, kidney cancer, head and neck tumors, and other solid tumors. CD200R, the homologous receptor for CD200, is also a member of IgSF. Inhibiting the binding of CD200, a potential immune checkpoint molecule, to CD200R could theoretically lead to tumor immunotherapy [39].

To further exploit the predictive power of the UAS in clinical potency, we further examined the relationship between scores and chemoradiotherapy signature (*AKR1C1*, *EGFR*, *MET*, *FLT3*, *KIT*, *SOX2*, *EZH2*, and *TBX5*). These genes inhibit the radiotherapy sensitivity of tumor cells by promoting DNA damage repairing and restraining cell death [40–42]. Upregulation of *AKR1C1* can diminish the production of reactive oxygen species and remove free radicals, resulting in reduced DNA damage, which confer chemotherapy resistance to cancer cells [42]. *EGFR* has been reported to reduce cellular sensitivity to radiotherapy in various solid tumors, thereby promoting tumor recurrence and metastasis [43].

OUTLIN has not been previously reported in GC; therefore, we chose it for experimental validation. The results from a set of functional experiments indicated that silencing OUTLIN could inhibit GC cell growth and cell viability, suggesting OUTLIN may be a potential target for GC treatment.

There were several limitations within our study. First, our proposed UAS was generated using public databases; therefore, additional large-scale prospective and multicenter clinical studies are necessary to verify our data. Furthermore, we only validated OUTLIN in the UAS using *in vitro* experiments. Further *in vivo* or molecular experiments are required to confirm the role of UAS in the future.

5. Conclusions

In this research, a prognostic signature based on five ubiquitination-associated genes was generated for the first time; the signature could serve as an independent prognostic factor for GC cases and mirror the immune landscape of GC. Our proposed signature can adequately forecast survival outcomes and evaluate the immunotherapy response of GC cases. Our data provide a valuable reference for GC detection and treatment.

Availability of Data and Materials

The public datasets to support the results of this subject can be gained from TCGA (<https://portal.gdc.cancer.gov/>) and GEO (<https://www.ncbi.nlm.nih.gov/geo/>).

Author Contributions

ZH and CP designed the study. ZZ collected the data. YT and HH analyzed the datasets and interpreted the results. ZH and CP performed experiments. FQ and HQ were responsible for conceptualization, synthesizing findings and drawing conclusions. All authors contributed to editorial changes in the manuscript. All authors read and approved the final manuscript. All authors have participated sufficiently in the work and agreed to be accountable for all aspects of the work.

Ethics Approval and Consent to Participate

Not applicable.

Acknowledgment

Not applicable.

Funding

This research received no external funding.

Conflict of Interest

The authors declare no conflict of interest.

Supplementary Material

Supplementary material associated with this article can be found, in the online version, at <https://doi.org/10.31083/j.fbl2811304>.

References

- [1] Global Burden of Disease 2019 Cancer Collaboration, Kocarnik JM, Compton K, Dean FE, Fu W, Gaw BL, *et al.* Cancer Incidence, Mortality, Years of Life Lost, Years Lived With Disability, and Disability-Adjusted Life Years for 29 Cancer Groups From 2010 to 2019: A Systematic Analysis for the Global Burden of Disease Study 2019. *JAMA Oncology*. 2022; 8: 420–444.
- [2] Quail DF, Joyce JA. Microenvironmental regulation of tumor progression and metastasis. *Nature Medicine*. 2013; 19: 1423–1437.
- [3] Bagaev A, Kotlov N, Nomic K, Svekolkina V, Gafurov A, Isaeva O, *et al.* Conserved pan-cancer microenvironment subtypes predict response to immunotherapy. *Cancer Cell*. 2021; 39: 845–865.e7.
- [4] Bader JE, Voss K, Rathmell JC. Targeting Metabolism to Improve the Tumor Microenvironment for Cancer Immunotherapy. *Molecular Cell*. 2020; 78: 1019–1033.
- [5] Geng R, Song J, Zhong Z, Ni S, Liu W, He Z, *et al.* Crosstalk of Redox-Related Subtypes, Establishment of a Prognostic Model and Immune Responses in Endometrial Carcinoma. *Cancers*. 2022; 14: 3383.
- [6] Aliabadi F, Sohrabi B, Mostafavi E, Pazoki-Toroudi H, Webster TJ. Ubiquitin-proteasome system and the role of its inhibitors in cancer therapy. *Open Biology*. 2021; 11: 200390.
- [7] Zhou X, Sun SC. Targeting ubiquitin signaling for cancer immunotherapy. *Signal Transduction and Targeted Therapy*. 2021; 6: 16.

- [8] Bsat S, Chanbour H, Bsat A, Alomari S, Moussalem C, Houshiemy MNE, *et al.* Clinical utility of degradomics as predictors of complications and clinical outcome in aneurysmal subarachnoid hemorrhage. *Journal of Integrative Neuroscience*. 2021; 20: 489–497.
- [9] Popovic D, Vucic D, Dikic I. Ubiquitination in disease pathogenesis and treatment. *Nature Medicine*. 2014; 20: 1242–1253.
- [10] Senft D, Qi J, Ronai ZA. Ubiquitin ligases in oncogenic transformation and cancer therapy. *Nature Reviews Cancer*. 2018; 18: 69–88.
- [11] Pang Y, Maxwell E, Sindrewicz-Goral P, Shapanis A, Li S, Morgan M, *et al.* Galectin-3 Is a Natural Binding Ligand of MCAM (CD146, MUC18) in Melanoma Cells and Their Interaction Promotes Melanoma Progression. *Biomolecules*. 2022; 12: 1451.
- [12] Tian M, Zhu R, Ding F, Liu Z. Ubiquitin-specific peptidase 46 promotes tumor metastasis through stabilizing ENO1 in human esophageal squamous cell carcinoma. *Experimental Cell Research*. 2020; 395: 112188.
- [13] Wilkerson MD, Hayes DN. ConsensusClusterPlus: a class discovery tool with confidence assessments and item tracking. *Bioinformatics*. 2010; 26: 1572–1573.
- [14] Mangiola S, Doyle MA, Papenfuss AT. Interfacing Seurat with the R tidy universe. *Bioinformatics*. 2021; 37: 4100–4107.
- [15] Newman AM, Liu CL, Green MR, Gentles AJ, Feng W, Xu Y, *et al.* Robust enumeration of cell subsets from tissue expression profiles. *Nature Methods*. 2015; 12: 453–457.
- [16] Geeleher P, Cox N, Huang RS. pRRophetic: an R package for prediction of clinical chemotherapeutic response from tumor gene expression levels. *PLoS ONE*. 2014; 9: e107468.
- [17] Mansour MA. Ubiquitination: Friend and foe in cancer. *The International Journal of Biochemistry & Cell Biology*. 2018; 101: 80–93.
- [18] Chen X, Kuang W, Zhu Y, Zhou B, Li X, Zhang X, *et al.* An E3 Ubiquitin Ligase RNF139 Serves as a Tumor-Suppressor in Glioma. *Journal of Molecular Neuroscience*. 2021; 71: 1664–1673.
- [19] Peng Y, Liu J, Wang Z, Cui C, Zhang T, Zhang S, *et al.* Prostate-specific oncogene OTUD6A promotes prostatic tumorigenesis via deubiquitinating and stabilizing c-Myc. *Cell Death and Differentiation*. 2022; 29: 1730–1743.
- [20] Yu L, Shen N, Shi Y, Shi X, Fu X, Li S, *et al.* Characterization of cancer-related fibroblasts (CAF) in hepatocellular carcinoma and construction of CAF-based risk signature based on single-cell RNA-seq and bulk RNA-seq data. *Frontiers in Immunology*. 2022; 13: 1009789.
- [21] Song J, Liu Y, Guan X, Zhang X, Yu W, Li Q. A Novel Ferroptosis-Related Biomarker Signature to Predict Overall Survival of Esophageal Squamous Cell Carcinoma. *Frontiers in Molecular Biosciences*. 2021; 8: 675193.
- [22] Han S, Wang R, Zhang Y, Li X, Gan Y, Gao F, *et al.* The role of ubiquitination and deubiquitination in tumor invasion and metastasis. *International Journal of Biological Sciences*. 2022; 18: 2292–2303.
- [23] Cockram PE, Kist M, Prakash S, Chen SH, Wertz IE, Vucic D. Ubiquitination in the regulation of inflammatory cell death and cancer. *Cell Death and Differentiation*. 2021; 28: 591–605.
- [24] Xie C, Powell C, Yao M, Wu J, Dong Q. Ubiquitin-conjugating enzyme E2C: a potential cancer biomarker. *The International Journal of Biochemistry & Cell Biology*. 2014; 47: 113–117.
- [25] Zhang HQ, Zhao G, Ke B, Ma G, Liu GL, Liang H, *et al.* Overexpression of UBE2C correlates with poor prognosis in gastric cancer patients. *European Review for Medical and Pharmacological Sciences*. 2018; 22: 1665–1671.
- [26] Lu ZN, Song J, Sun TH, Sun G. UBE2C affects breast cancer proliferation through the AKT/mTOR signaling pathway. *Chinese Medical Journal*. 2021; 134: 2465–2474.
- [27] Ikeda F. Linear ubiquitination signals in adaptive immune responses. *Immunological Reviews*. 2015; 266: 222–236.
- [28] Wang W, Li M, Ponnusamy S, Chi Y, Xue J, Fahmy B, *et al.* ABL1-dependent OTULIN phosphorylation promotes genotoxic Wnt/ β -catenin activation to enhance drug resistance in breast cancers. *Nature Communications*. 2020; 11: 3965.
- [29] Yuan P, Feng Z, Huang H, Wang G, Chen Z, Xu G, *et al.* USP1 inhibition suppresses the progression of osteosarcoma via destabilizing TAZ. *International Journal of Biological Sciences*. 2022; 18: 3122–3136.
- [30] Li N, Wu L, Zuo X, Luo H, Sheng Y, Yan J. USP1 Promotes GC Metastasis via Stabilizing ID2. *Disease Markers*. 2021; 2021: 3771990.
- [31] Ma A, Tang M, Zhang L, Wang B, Yang Z, Liu Y, *et al.* Correction to: USP1 inhibition destabilizes KPNA2 and suppresses breast cancer metastasis. *Oncogene*. 2022; 41: 1673.
- [32] Wu H, Huang M, Lu M, Zhu W, Shu Y, Cao P, *et al.* Regulation of microtubule-associated protein tau (MAPT) by miR-34c-5p determines the chemosensitivity of gastric cancer to paclitaxel. *Cancer Chemotherapy and Pharmacology*. 2013; 71: 1159–1171.
- [33] Zhu L, Chen Z, Guo T, Chen W, Zhao L, Guo L, *et al.* USP2 Inhibits Lung Cancer Pathogenesis by Reducing ARID2 Protein Degradation via Ubiquitination. *BioMed Research International*. 2022; 2022: 1525216.
- [34] Topalian SL, Taube JM, Anders RA, Pardoll DM. Mechanism-driven biomarkers to guide immune checkpoint blockade in cancer therapy. *Nature Reviews Cancer*. 2016; 16: 275–287.
- [35] Wherry EJ, Kurachi M. Molecular and cellular insights into T cell exhaustion. *Nature Reviews Immunology*. 2015; 15: 486–499.
- [36] Segal NH, Ou SHI, Balmanoukian A, Fury MG, Massarelli E, Brahmer JR, *et al.* Safety and efficacy of durvalumab in patients with head and neck squamous cell carcinoma: results from a phase I/II expansion cohort. *European Journal of Cancer*. 2019; 109: 154–161.
- [37] Gu H, Song J, Chen Y, Wang Y, Tan X, Zhao H. Inflammation-Related LncRNAs Signature for Prognosis and Immune Response Evaluation in Uterine Corpus Endometrial Carcinoma. *Frontiers in Oncology*. 2022; 12: 923641.
- [38] Ma Y, Zhang Z, Chen R, Shi R, Zeng P, Chen R, *et al.* NRP1 regulates HMGB1 in vascular endothelial cells under high homocysteine condition. *American Journal of Physiology. Heart and Circulatory Physiology*. 2019; 316: H1039–H1046.
- [39] Choe D, Choi D. Cancel cancer: The immunotherapeutic potential of CD200/CD200R blockade. *Frontiers in Oncology*. 2023; 13: 1088038.
- [40] Kang YK, Chen LT, Ryu MH, Oh DY, Oh SC, Chung HC, *et al.* Nivolumab plus chemotherapy versus placebo plus chemotherapy in patients with HER2-negative, untreated, unresectable advanced or recurrent gastric or gastro-oesophageal junction cancer (ATTRACTION-4): a randomised, multicentre, double-blind, placebo-controlled, phase 3 trial. *The Lancet Oncology*. 2022; 23: 234–247.
- [41] Recondo G, Che J, Jänne PA, Awad MM. Targeting MET Dysregulation in Cancer. *Cancer Discovery*. 2020; 10: 922–934.
- [42] Zeng CM, Chang LL, Ying MD, Cao J, He QJ, Zhu H, *et al.* Aldo-Keto Reductase AKR1C1-AKR1C4: Functions, Regulation, and Intervention for Anti-cancer Therapy. *Frontiers in Pharmacology*. 2017; 8: 119.
- [43] Martínez P, Mak RH, Oxnard GR. Targeted Therapy as an Alternative to Whole-Brain Radiotherapy in EGFR-Mutant or ALK-Positive Non-Small-Cell Lung Cancer With Brain Metastases. *JAMA Oncology*. 2017; 3: 1274–1275.